American Mineralogist, Volume 77, pages 725–740, 1992

The temperature dependence of the cation distribution in magnesioferrite ($MgFe_2O_4$) from powder XRD structural refinements and Mössbauer spectroscopy

H. St.C. O'Neill, H. Annersten,* D. Virgo**
Bayerisches Geoinstitut, Universität Bayreuth, W-8580 Bayreuth, Germany

Abstract

Magnesioferrite ($MgFe_2O_4$ spinel) was synthesized in equilibrium with excess MgO using a flux method. Chemical analysis shows that the $MgFe_2O_4$ is stoichiometric, within analytical uncertainty. Samples were annealed at intervals of 50 °C between 450 and 1250 °C and quenched in H_2O. The time needed to reach equilibrium at low temperatures (450–650 °C) was assessed by monitoring the change of lattice parameter (a_0) with time. In addition, the changes in a_0 at 550–650 °C were reversed, using material annealed at 400 °C for 50 d. Some samples were further characterized by measuring their Néel temperatures, using DSC.

The cation distributions in the quenched samples were determined using both powder X-ray diffraction and Mössbauer spectroscopy. To increase the resolution in the latter, the samples were studied in an applied magnetic field of 4.5 T at 12–171 K. The cation distribution changes smoothly with temperature, with the cation inversion parameter (x) decreasing from 0.90 at 450 °C to 0.72 at 1100 °C. The precision with which x can be determined is ±0.004 from XRD and ~±0.01 from the Mössbauer spectroscopy. The two sets of measurements agree well with each other, the mean difference in x being 0.0056 ± 0.0102. Thermodynamic modeling shows that the cation distribution can be described with a nonlinear enthalpy of disordering model, with $\alpha^{Mg\text{-}Fe^{3+}} = 26.6 \pm 0.4$ and $\beta = -21.7 \pm 0.3$ kJ/g-atom. Incorporation of a small excess (nonconfigurational) entropy term into the model gives a slightly better fit, however. The disordering in $MgFe_2O_4$ as a function of temperature is virtually identical to that found in Fe_3O_4 from thermopower measurements.

The present results differ to a greater or lesser extent from most of the previous work on $MgFe_2O_4$. This is most likely attributable to differences in stoichiometry. We also present some results on nonstoichiometric "$MgFe_2O_4$," i.e., solutions of $MgFe_2O_4$ and γ-Fe_2O_3, which tend to confirm this hypothesis, at least for some of the earlier studies.

Introduction

Simple, stoichiometric oxide spinels have a general formula that may be written $^{[4]}(A_{1-x}B_x)^{[6]}(A_xB_{2-x})O_4$, where x is the inversion parameter. Much of the crystal-chemical interest in the spinel structure stems from the common ability, indicated in the above formula, of the two different cations to disorder over the two cation sites. The thermodynamics of this phenomenon has been discussed many times, e.g., O'Neill and Navrotsky (1983, 1984), which contains references to earlier work. A brief summary will be given here. The ideal configurational entropy of the spinel is

$$S_{conf} = -R\left[\sum nX_N \ln(X_N)\right] \quad (1)$$

where X_N is the fraction of cations of type N in each kind of site, n is the number of sites per formula unit (i.e., three), and the summation is over all sites. At equilibrium, the free energy will be at a minimum with respect to the degree of inversion—i.e., $(\partial \Delta G/\partial x)_{T,P,N\ldots} = 0$. Since

$$\left(\frac{\partial S_{conf}}{\partial x}\right)_{T,P,N\ldots} = -R \ln\left(\frac{x^2}{(1-x)(2-x)}\right) \quad (2)$$

this gives:

$$RT \ln\left(\frac{x^2}{(1-x)(2-x)}\right) = \left(\frac{\partial \Delta G_D}{\partial x}\right)_{T,P,N\ldots} \quad (3)$$

where ΔG_D is the change in nonconfigurational free energy of disordering. O'Neill and Navrotsky (1983, 1984) suggested that this term would be mainly an enthalpy term (at least for spherically symmetrical cations) and was a quadratic function of x:

$$\Delta G_D = \alpha x + \beta x^2. \quad (4)$$

* Permanent address: Department of Mineralogy and Petrology, Institute of Geology, University of Uppsala, Box 555, S-75122 Uppsala, Sweden.
** Permanent address: Geophysical Laboratory, Carnegie Institution of Washington, Washington, DC 20015, U.S.A.

0003–004X/92/0708–0725$02.00

They furthermore suggested that the β term might be in the region of -15 to -25 kJ/mol for most 2-3 spinels. The importance of this nonlinear enthalpy of disordering is that the site preference of a particular cation (octahedral or tetrahedral) may depend on the degree of inversion of the spinel into which it is substituting. This can have profound effects for the pattern of site occupancies across a solid solution, in particular, between a largely normal and a largely inverse spinel, and consequently for the thermodynamic properties (i.e., activity-composition relations) of such a system, as well as all the many physical properties that depend on the cation distribution.

The experimental basis for this proposed nonlinear enthalpy of disordering in simple spinels was actually not very extensive. O'Neill and Navrotsky (1983) were able to find data on the change of cation distribution with temperature for only seven spinels against which they could test the predictions of their model. Prominent among these was magnesioferrite, $MgFe_2O_4$, since no less than six studies were available (see, e.g., Table 1). This, however, proved to be an embarassment of riches, for although all agreed that $MgFe_2O_4$ was a largely inverse spinel that showed a substantial change in cation distribution with temperature, in detail there was enough variation in the results to produce very different values for the calculated α and β parameters. Indeed, the values for the important β parameter varied from 0 to -18 kJ/mol (O'Neill and Navrotsky, 1983, their Table 5).

To resolve these discrepancies, we have studied again the temperature dependence of the cation distribution in well-characterized $MgFe_2O_4$, using two independent methods, powder XRD and Mössbauer spectroscopy.

Stoichiometry in $MgFe_2O_4$

The biggest difficulty in synthesizing $MgFe_2O_4$ is control of the stoichiometry. $MgFe_2O_4$ may depart from the stoichiometric ideal in three directions: (1) substitution of Fe^{2+} for Mg, causing solid solution toward Fe_3O_4; (2) solid solution toward γ-Fe_2O_3 (maghemite); and (3) excess MgO. The first two mechanisms are well established possibilities under certain conditions; evidence for the importance of the last is equivocal, and will be reviewed below.

First, consider deviations toward an Fe_3O_4 component. Nominally stoichiometric $MgFe_2O_4$ may partially decompose to a Fe_3O_4-containing solid solution according to the reaction

$$\underset{\text{spinel}}{6\ MgFe_2O_4} = \underset{\text{spinel}}{4\ Fe_3O_4} + \underset{\text{oxide (or spinel)}}{6\ MgO} + O_2. \quad (5)$$

At constant f_{O_2}, such as that of air, Reaction 5 goes progressively more to the right side with increasing temperature. The minimum amount of Fe_3O_4 in the spinel occurs when the activity of MgO is unity; with that assumption, ideal mixing between $MgFe_2O_4$ and Fe_3O_4, and $f_{O_2} = 0.2$ (air), the thermodynamic data given in Robie et al. (1978) for the components in Reaction 5 may be used to predict $X_{Fe_3O_4}$ as 1000 K, 1.2×10^{-4}; 1200 K, 1.9×10^{-3}; 1400 K, 0.012; 1600 K, 0.050. The value of S^0_{298} for $MgFe_2O_4$, given in Robie et al. (1978), contains an extra R ln 2 for the zero-point entropy; we have added a further R ln 2 to give a net zero point entropy of 2R ln 2, appropriate for the configurational entropy of a completely inverse spinel. The actual configurational entropy of a sample quenched from $T > 0$ K will be even somewhat larger.

It should only be possible to synthesize something approaching stoichiometric $MgFe_2O_4$ at relatively low temperatures, at least in air (for example, for $X_{Fe_3O_4}$ to be below 0.5%, the synthesis temperature should be less than 1000 °C). Since the thermodynamic data for "$MgFe_2O_4$" was itself obtained from material synthesized at higher temperatures and was therefore almost certainly nonstoichiometric, these calculations should only be regarded as approximate; furthermore, if the activity of MgO is lowered from unity by also substituting into the spinel (by some defect mechanism), then Reaction 5 would move toward the right, and $X_{Fe_3O_4}$ will be even larger. In this case, the synthesis product would appear as single-phase

Table 1. A summary of previous investigations of the cation distribution in $MgFe_2O_4$ spinel

Reference	Method*	T range (°C)/no. of samples**	Comments†
Bertaut (1951)	XRD	20(?)–1200/4	
Pauthenet and Bochirol (1951)	SM	640–1200/10	
Kriessman and Harrison (1956)	SM	440–1400/8	also XRD(a_0), NS
Epstein and Frackiewicz (1958)	SM	600–1200/?	eqn. only, some rate data, θ_c
Mozzi and Paladino (1963)	SM, XRD(a_0,x,u)	410–1100/6 + 3	claimed NS, probably stoic!
Agranovskaya and Saksonov (1966)	SM, XRD(a_0,x)	1100, sc/2	
Allen (1966)	XRD(a_0,x)	345–1650/27	
Tellier (1967)	SM	500–1200/sc	also XRD(a_0), θ_c, NS
Sawatsky et al. (1969)	Möss‡	1250+, sc/2	
Faller and Birchenall (1970)	XRD	700–1254/9	NS, some data at T
De Grave et al. (1975)	XRD(a_0,x)	1100, sc/2	NS
Babaev et al. (1976)	ND(a_0,x,u)	1300/1	quenched? NS?

* SM = saturation magnetization; XRD = powder X-ray diffraction; ND = neutron diffraction.
** The designation sc refers to slowly cooled or furnace cooled.
† NS: reason to suspect nonstoichiometry, usually from a_0 or θ_c (Curie temperature)—see text.
‡ Also measurements in applied magnetic field.

spinel (i.e., no excess MgO). Note that small amounts of excess MgO would be extremely difficult to detect. With X-ray diffraction, all the main MgO reflections coincide with $MgFe_2O_4$ reflections, so that amounts of MgO less than about 2% by weight would remain completely hidden. The amount of MgO produced at 1600 K, according to the above calculation, is only 1.5 wt%.

Empirical determinations (by wet chemistry) of the FeO content of "$MgFe_2O_4$" synthesized in air agree reasonably well with the above calculations, despite these uncertainties. For compositions in equilibrium with excess MgO, Paladino (1960) found no FeO component in air at 1000 and 1100 °C but found 0.3–0.6 wt% at 1200 °C. At 1300 °C in air, Ulmer and Smothers (1968) found 1.04 wt% FeO, corresponding to $X_{Fe_3O_4} = 0.03$, if the "$MgFe_2O_4$" is assumed to lie exactly on the $MgFe_2O_4$-Fe_3O_4 join. Our calculation gives $X_{Fe_3O_4} = 0.045$ under these conditions.

The lattice parameter of stoichiometric Fe_3O_4 is 8.397 Å; since those of stoichiometric $MgFe_2O_4$ vary around this value (i.e., 8.38–8.40 Å—see below), it is not possible to use lattice parameter measurements to test for Fe_3O_4 substitution in $MgFe_2O_4$. Conversely, a lattice parameter outside that range might indicate other types of nonstoichiometry.

Typically, 2-3 spinels of the type AB_2O_4 may show considerable solid solution toward the B_2O_3 component at high temperatures, provided that the B cation is not one with a large octahedral site preference energy (e.g., where B is Fe^{3+}, Al, Ga, but not Cr or Rh). Some such systems have been investigated extensively and are well characterized (e.g., $MgAl_2O_4$-γ-Al_2O_3, Navrotsky et al., 1986; Fe_3O_4-γ-Fe_2O_3, Dieckmann, 1982). The lattice parameter of γ-Fe_2O_3 is 8.339 Å (Lindsley, 1976); hence solid solution of γ-Fe_2O_3 in $MgFe_2O_4$ should result in a lowering of the $MgFe_2O_4$ lattice parameter and should therefore be readily detectable. It is also possible that a Fe_3O_4 component, originally produced by high-temperature decomposition of stoichiometric $MgFe_2O_4$ according to Reaction 5, may oxidize at lower temperatures, yielding this type of nonstoichiometry.

The substitution of an excess B_2O_3 component in spinel occurs by a cation vacancy mechanism. In contrast, solid solution toward the AO component would have to occur either by cation interstitials or by O vacancies, if charge balance is to be maintained. Such properties as the extent, temperature dependence, and quenchability of this type of defect spinel might therefore be expected to be quite different. Actually, whether or not significant excess MgO can substitute into $MgFe_2O_4$ is a matter of some contention. Schmalzried (1961) showed that there was negligible excess NiO in $NiAl_2O_4$ and CoO in $CoAl_2O_4$ and only slight solution of MgO in $MgGa_2O_4$ (1000–1400 °C). O'Neill (unpublished data) has confirmed that for $NiAl_2O_4$ and $CoAl_2O_4$, as well as for $ZnAl_2O_4$, but also found negligible excess MgO in $MgGa_2O_4$ at temperatures near 1000 °C. The indication is that any excess AO component is usually present in amounts too low to detect.

Recently, however, Tamaura and Tabata (1990) prepared metastable cation-excess magnetite ($Fe_{3+\delta}O_4$, $\delta = 0.127$) with $a_0 = 8.418$ Å, which is significantly larger than that for stoichiometric magnetite (8.397 Å). The equilibrium solubility of excess FeO in Fe_3O_4 at temperature (that is, rather than in quenched specimens) has been considered several times, e.g., the extensive and internally consistent thermogravimetric study of Dieckmann (1982). The nonstoichiometry occurs by means of cation interstitials, not O vacancies (Dieckmann and Schmalzried, 1977). Extrapolation of Dieckmann's model for the cation interstitial substitution in Fe_3O_4 to the Fe_3O_4 + "FeO" phase boundary shows that the maximum O/Fe ratio is 1.330–1.332 in the temperature range 900–1400 °C (stoichiometry is at O/Fe = $\frac{4}{3}$ = 1.333). This corresponds to a molar FeO/Fe_2O_3 ratio of 1.01/1.03. Even these small values are probably maximum estimates, due to the nature of the extrapolation—see Figures 2 and 3 in Dieckmann (1982).

From the above evidence, we suggest that AO-excess type of nonstoichiometry in spinels is generally rather small, and, judging from the Fe_3O_4 data, will probably not exceed about 2% at temperatures less than 1400 °C. We have also not been able to find any firm evidence for thermodynamically stable O vacancies in oxide spinels.

The possible ways in which $MgFe_2O_4$ might be expected to deviate from stoichiometry are clearly complex. Unfortunately, existing studies of the actual behavior of $MgFe_2O_4$ at high temperatures do not entirely clarify the picture, as they are mutually contradictory. For example, Blackman (1959) reports no perceptible dissociation from nominally pure $MgFe_2O_4$ up to 1688 K, contrary to the expectations from thermodynamic data, but does report weight loss from a specimen with bulk excess MgO. Why this should be so is difficult to explain, and is anyway challenged by the results of Paladino (1960), which are further notable for two reasons: first, that they indicate that there may actually be no field of stability for truly stoichiometric $MgFe_2O_4$; and, second, that considerable excess MgO may indeed dissolve in the structure. That led Mozzi and Paladino (1963) to claim that the spinel used in their cation distribution study had the formula $Mg_{1.06}Fe_{1.94}O_{3.97}$ (i.e., molar $MgO/Fe_2O_3 = 1.09$, or a total cation to O ratio of 0.773 ± 0.001, cf. 0.75 for stoichiometry). In fact, as shown below, the results of Mozzi and Paladino are very similar to our own on (virtually) stoichiometric $MgFe_2O_4$. The simplest explanation for this is that the apparent deviation from stoichiometry found by Paladino (1960) is an artifact caused by a weighing error; that seems plausible given the rather convoluted method of sample preparation described by Paladino—decomposition from a precipitate of the mixed oxalates, the compositions being corrected, it may be noted, for "the fact that precipitation was not quantitative." In support of this proposition, we note that Katsura and Kimura (1965) and Speidel (1967) obtained total cation to O ratios of 0.752 ± 0.002 and 0.750 ± 0.001 for Mg-Fe_2O_4-Fe_3O_4 solid solutions coexisting with magnesiowüstite at 1160 and 1300 °C, respectively.

Synthesis and sample characterization

In view of all this uncertainty and the variation among previous studies in the reported properties of $MgFe_2O_4$, it was felt to be particularly desirable first to synthesize $MgFe_2O_4$ at a sufficiently low temperature to avoid the FeO complication; second, to ensure that there is no excess Fe_2O_3 component by using excess MgO, adopting the view, for the reasons discussed above, that nonstoichiometry in this direction is negligible at moderate temperatures; and third, and most important, to check the products of the synthesis by direct chemical analysis.

Attempts to synthesize $MgFe_2O_4$ at $T < 950$ °C from oxide mixes gave a relatively poorly crystallized experimental product, with incomplete reaction. Hydrothermal synthesis has the problem of maintaining the requisite high f_{O_2}. Accordingly, $MgFe_2O_4$ was synthesized in air, using a flux. A mixture of 2 g of MgO, 4 g of Fe_2O_3, 20 g of Na_2WO_4, and 2 g of WO_3 were ground together under acetone in an agate mortar and loaded into a 50-mL Pt crucible with a lid. Note that this composition contains MgO in excess of the amount needed to form stoichiometric $MgFe_2O_4$. The mixture was melted at 1260 °C and then cooled at a controlled rate of 6 °C per hour to either 950 (first batch) or 900 °C (second batch), at which temperature it was held for approximately 12 h. The subsequent work showed that the two batches appeared in all respects identical to each other. The crucible and contents were then removed from the furnace and allowed to cool to room temperature. The sodium tungstate flux was removed by dissolution in warm H_2O, aided by shaking in an ultrasonic bath. The H_2O was decanted off and replaced several times, which also removed any fine-grained material. The product consisted of euhedral octahedra of reddish brown magnesioferrite spinel about 10 μm across, which were translucent in a grain mount made with refractive index oils, plus some white cubes of MgO (completely colorless in the oil mount), with an edge length of 10–20 μm. Nearly every MgO crystal contained a few (typically one to three) small (<2 μm) inclusions of $MgFe_2O_4$, but the $MgFe_2O_4$ crystals were inclusion free. Some of this MgO-containing material was reserved for electron microprobe analysis; the rest was washed in dilute nitric acid to remove the MgO, leaving single-phase spinel.

An initial attempt at flux synthesis used the recipe of Kunnmann et al. (1965), with 1.65 g of MgO, 6.0 g of Fe_2O_3, 20 g of Na_2WO_4, and 3.4 g of WO_3 (i.e., a stoichiometric MgO/Fe_2O_3 ratio), cooled at 12 °C/h from 1280 to 1000 °C. This produced relatively large euhedral crystals of hematite (α-Fe_2O_3), up to 500 μm across, and crystals, 5–15 μm across, of what proved to be nonstoichiometric magnesioferrite. Nearly all of the α-Fe_2O_3 could be removed with a 63-μm sieve, although a few smaller (5 μm) but euhedral hexagonal prisms could still be observed. The remaining spinel was black in color, and very dark brown (almost completely opaque) under the refractive index oils. This nonstoichiometric magnesioferrite was used in a few subsequent experiments, mainly to see if the discrepancies between the results of this study and the earlier work could be explained by differences in stoichiometry.

Aliquots of 40–100 mg of these materials were annealed at temperatures from 400 to 1250 °C in air, in unsealed Pt capsules, and quenched in H_2O as described in O'Neill et al. (1991).

Chemical analysis

The acid-cleaned stoichiometric $MgFe_2O_4$ was analyzed by ICP at the Geophysical Laboratory, using Specpure $MgFe_2O_4$ supplied by Johnson Matthey as a standard. Results (in weight percent) are 20.46 ± 0.29 for MgO and 79.95 ± 0.95 for Fe_2O_3, summing to 100.4%. This corresponds to a molar ratio of MgO/Fe_2O_3 of 1.014 ± 0.019—that is, stoichiometric within analytical error. No Na or W could be detected.

Both the stoichiometric and nonstoichiometric materials were analyzed by electron microprobe at the Bayerisches Geoinstitut, using a Cameca SX50 in the wavelength-dispersive mode. Standards of synthetic Fe_2O_3 and both $MgAl_2O_4$ and Mg_2SiO_4 were used; the results from the two MgO standards were identical. The average from 19 analyses of stoichiometric $MgFe_2O_4$ was MgO 20.50 ± 0.16 and Fe_2O_3 80.09 ± 0.40 wt%, sum 100.59%, molar $MgO/Fe_2O_3 = 1.014 \pm 0.009$. The coexisting periclase had MgO 97.87 ± 0.18, Fe_2O_3 1.76 ± 0.08 (total 99.63%, $N = 5$); this Fe content is noticeably less than the 9 wt% Fe_2O_3 in MgO, coexisting with $MgFe_2O_4$ at 1300 °C in air, reported by Ulmer and Smothers (1968). In agreement with the ICP bulk analyses, no Na or W could be detected by the microprobe.

The nonstoichiometric magnesioferrite had MgO 16.38 ± 0.37, Fe_2O_3 84.84 ± 0.64, total 101.2 wt% ($N = 23$). This gives molar $MgO/Fe_2O_3 = 0.765 \pm 0.021$ (i.e., a solid solution of 76.5% $MgFe_2O_4$ and 23.5% γ-Fe_2O_3, neglecting a probable small amount of Fe^{2+}).

The acid-cleaned stoichiometric magnesioferrite was also analyzed at the University of Uppsala with a Cameca SX50 electron microprobe, using standards of synthetic MgO and Fe_2O_3. Results from 14 analyses on grains larger than 10 μm in diameter, with totals in the range 98–100.5%, are MgO 20.35 ± 0.25 and Fe_2O_3 78.44 ± 0.53 wt%, sum 98.8%, molar MgO/Fe_2O_3 ratio 1.028 ± 0.015.

There is an indication in the above results that our stoichiometric $MgFe_2O_4$ may actually be slightly MgO rich. If so, it may be noted that no excess MgO was observed to exsolve even during long equilibration times at lower temperatures, unlike, for example, the clear evidence, presented below, for exsolution of α-Fe_2O_3 from the nonstoichiometric "$MgFe_2O_4$." In what follows, we will assume ideal stoichiometry.

Lattice parameter measurements

Lattice parameters were measured using Co$K\alpha_1$ radiation ($\lambda = 1.78897$ Å) on a STOE focusing diffractometer with a curved Ge monochromator (see O'Neill et al.,

1991). All samples were measured with an internal standard of NBS Si (a_0 = 5.43081, corrected from the recommended 5.43094 at 298.1 K for Cu$K\alpha_1$ = 1.5405981 to the value of Cu$K\alpha_1$ used in our laboratory, 1.54056). The diffraction pattern was collected from 40 to 120° 2θ, using ½° increments of the position-sensitive detector. Proprietary software from STOE was used to determine peak positions by fitting entire peak profiles. The six main Si peaks in the 2θ range covered were used to derive a two-term (linear) correction to the observed 2θ. The spinel lattice parameter, a_0, was then determined by a weighted nonlinear least-squares refinement of the positions of the ten most intense spinel peaks. The mean internal estimate of the standard deviation of a_0, calculated from over a hundred such determinations, is 0.00007 Å, corresponding to a standard deviation in the corrected 2θ values of 0.003°. However, the main sources of error in the measurements are caused by variations in room temperature and the differences in thermal expansion of Si and magnesioferrite. Taking that into account, we estimate a more realistic uncertainty of ±0.00015 (1 sd). An external estimate of the standard deviation may be obtained from three series of determinations of a_0, from different samples equilibrated at 600, 650, and 700 °C for various lengths of time, but with all times in excess of that required for equilibration—see Figure 1. These data provide estimates of the uncertainty in a_0 of ±0.00011–0.00013.

Lattice parameters for samples annealed and then quenched at intervals of 50 °C from 450 to 1250 °C are listed in Table 2 and shown in Figure 2. The increase in a_0 with temperature of annealing reflects increasing disorder ($x \rightarrow \frac{2}{3}$), caused by the systematic difference in both the sizes of the Mg and Fe^{3+} cations and the ratio of their sizes in tetrahedral vs. octahedral coordination (O'Neill and Navrotsky, 1983). Since the lattice parameter of a spinel is relatively easy to measure accurately and unambiguously and since it is potentially an extremely sensitive indicator of the cation distribution (in $MgFe_2O_4$,

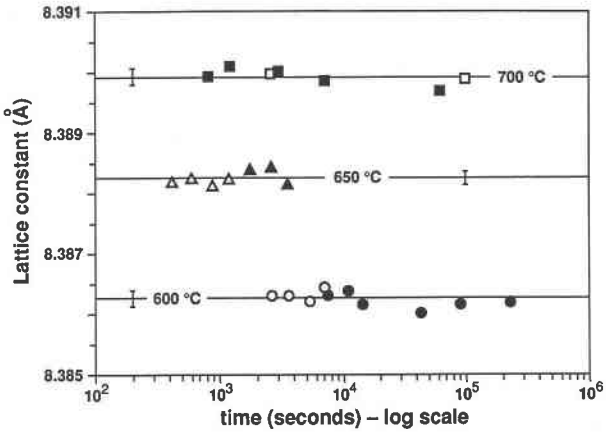

Fig. 1. Precision and reversibility of $MgFe_2O_4$ lattice parameter (a_0) measurements at 25 °C, on samples annealed at 600, 650, and 700 °C for various times, all long enough for equilibrium to be achieved. Solid symbols = starting material equilibrated at 950 °C; open symbols = experiments at 700 °C, starting material annealed at 1150 °C; experiments at 600 and 650 °C, reversals with material annealed at 400 °C for 50 d.

±0.0001 Å in a_0 corresponds to roughly ±0.001 in x—see below), it provides a ready means of characterizing the changes in cation distribution during different experimental conditions—the time needed to reach equilibrium, for example. That is, provided constant stoichiometry is maintained, for the lattice parameter may also be a sensitive indicator of that.

Equilibration times for the lowest temperatures (450–700 °C) were checked by following the change in a_0 with time until no further variation occurred. An example of such an a_0 vs. time curve is shown in Figure 3—these and similar kinetic results at other temperatures will be discussed in detail elsewhere (O'Neill, in preparation). In addition, equilibrium was verified by using some material slowly cooled and then annealed at 400 °C for 50 d to reverse the direction of approach to equilibrium at

Table 2. Lattice parameter measurements at 25 °C on $MgFe_2O_4$, annealed at temperatures from 400 to 1250 °C, and quenched into H_2O

Anneal T (°C)	No. of samples	Time	a_0 (Å)	Anneal T (°C)	No. of samples	Time	a_0 (Å)
400	1	50 d	8.3805	850	1	40 h	8.3946
450	1*	30 d	8.3806	900	1	24 h	8.3959
500	4*	52 h–8 d	8.3827	950	1	16 h	8.3970
550	5**	7–24 h	8.3845	1000	2	9 min and 12 h	8.3981
600	10**	3–64 h	8.3863	1050	2	5 and 35 min	8.3987
650	7**	10 min–1 h	8.3883	1100	1†	5 min	8.3998
700	7	15 min–10 d	8.3899	1150	1‡	5 min	8.4000
750	2	2 h	8.3914	1200	1	5 min	8.3998
800	1	45 h	8.3934	1250	1	5 min	8.4002

Note: All times are long enough for the cation distribution to have reached equilibrium (except at 400 °C). Where more than one sample was measured, a mean is given. Uncertainty is ±0.0003, 2 sd.

* Studied by following the change of a_0 with time, see O'Neill (in preparation).

** As above, but also reversed using material at 400 °C.

† Maximum value (after 5 min)—longer anneal times seemed to yield slightly lower values, e.g., 8.3989 after 25 min. This is probably related to stoichiometry, reflecting O-deficiency defects either directly or through faster reequilibration during the quench.

‡ A larger batch gave 8.3991 after 45 min.

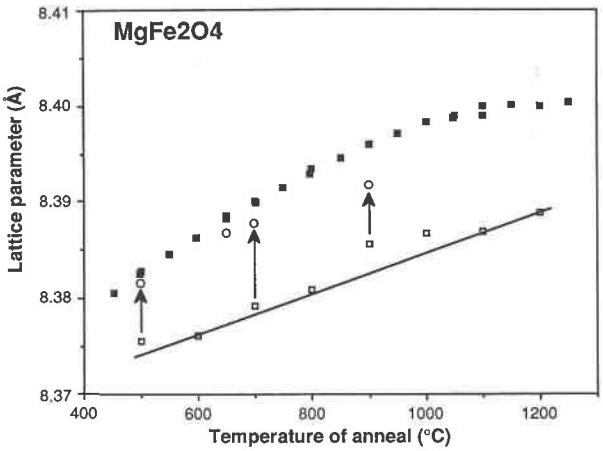

Fig. 2. Lattice parameter (a_0) measurements on quenched samples of stoichiometric $MgFe_2O_4$ (solid squares) and nonstoichiometric $MgFe_2O_4$ (open squares and circles). For the nonstoichiometric $MgFe_2O_4$ experiments, the starting material was initially annealed at 1100 °C and rapidly quenched. The samples plotted as open squares were then annealed for comparatively short times (series A), allowing the Mg/Fe^{3+} (± vacancy) distribution to equilibrate. This trend is shown by the straight line (drawn by eye). Longer annealing times result in a steady increase of a_0 as excess Fe_2O_3 exsolves as α-Fe_2O_3; final values are plotted as open circles (series B). A detailed view of the trend at 500 °C (series C) is given in Figure 3. Note that the deviation of many of the open squares from the indicated trend is due to incipient exsolution of Fe_2O_3 rather than errors in a_0 measurement; the accuracy of this is comparable to the size of the symbols.

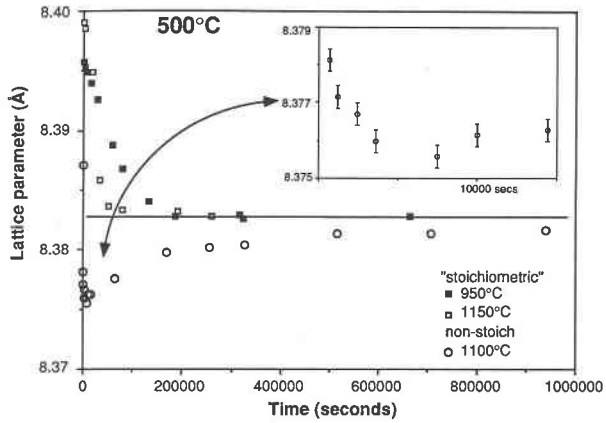

Fig. 3. A detailed look at the rate of equilibration of three samples of "$MgFe_2O_4$" during isothermal annealing at 500 °C, using the change of a_0 with time. All samples quenched in H_2O. Series 1 (filled squares): stoichiometric $MgFe_2O_4$, using material from batch 2 (removed from furnace after cooling to 900 °C; a_0 = 8.3957 Å, three separate measurements), thought to contain minimal defects. This series shows a straightforward and smooth approach to a steady value. Series 2 (open squares): same stoichiometric $MgFe_2O_4$ but heated to 1150 °C for 45 min, which darkens the material—this may reasonably be supposed to be due to some O loss (i.e., according to Eq. 4 in the text); a_0 is 8.3991 Å (two measurements), which is slightly but significantly less than the 8.4000 Å found for a sample quenched after just 5 min at the same temperature. This series shows a much faster change of a_0 with time initially, but the final value is the same as for the starting material annealed at 950 °C. Series C (open circles): nonstoichiometric "$MgFe_2O_4$" (23.5% Fe_2O_3).

550–700 °C (i.e., disordering experiments). With our starting material, it takes about 30 d for the cation distribution to reach equilibrium at 450 °C and less than 5 min at 700 °C.

At high temperatures, two problems arise: nonstoichiometry, as discussed above, and whether the quench rate is fast enough to preserve the equilibrium cation distribution during the quench. As to the first problem, we offer the following observations:

1. Material annealed at 1000 °C and below preserved the reddish brown color of the original synthesis, whereas the samples annealed at 1100 °C and above became much darker, although they still appeared translucent in the RI oil grain mount. The same phenomenon was observed by Allen (1966). The status of the two samples held at 1050 °C is hard to judge, but most observers think that they appear slightly darker.

2. Some of this dark material, quenched from 1150 °C, was then reannealed at 500, 700, and 900 °C. The lattice parameters for these reequilibrated samples were identical to those obtained from the original synthesis material at the same temperature (e.g., Figs. 1, 3), and the original red-brown color returned. However, the rate at which a_0 approached equilibrium at 500 °C was noticeably faster—see Figure 3.

3. No trace of exsolved MgO could be discerned in the XRD patterns of the samples held at 1100–1250 °C, nor could any be found by optical examination. These negative observations should not be taken to be definitive, as the amounts of MgO which might reasonably be expected to appear, for example by means of Reaction 5, would possibly be insufficient to be detected by these methods.

In conclusion, the dark color provides circumstantial evidence for some nonstoichiometry appearing in $MgFe_2O_4$ at 1100 °C and above, but we are not able to ascertain the exact nature or extent of it, except that the extent is not large.

The problem of maintaining the equilibrium cation distribution in $MgFe_2O_4$ during quenching from high temperatures was investigated by Faller and Birchenall (1970) by comparing cation distributions measured by powder XRD methods on quenched samples with those determined at temperature. They found good agreement between the two sets of experiments below ~1000 °C, but a sample quenched from 1250 °C showed an anomalous distribution, being no different from that at 1000 °C. The implication is that the rate of quenching was not fast enough to prevent some reequilibration. However, the exact method of quenching is not described, and, as will be argued below, the samples used by Faller and Birchenall have low lattice parameters, consistent with their being somewhat nonstoichiometric, and conse-

quently likely to reorder more rapidly (as demonstrated in the next section). It is therefore doubtful if their results are applicable to our study.

Figure 2 shows that there is little increase in a_0 of the (nominally) stoichiometric samples quenched from 1050 °C and above. It might be thought that this is evidence for insufficient quenching rates at these high temperatures; but there is also the problem of nonstoichiometry, and, as will be shown later, the thermodynamic model established from a fit to the cation distribution data obtained only on those samples annealed at 1000 °C and below actually predicts that there will be little change in the cation distribution with temperature above 1100 °C. Finally, we do see a small but statistically significant change in the lattice constant of the nonstoichiometric material above 1000 °C, even though the rate of ordering at lower temperatures is faster in this material (e.g., Fig. 3). However, this increase may also have other causes, such as a greater Fe_3O_4 component (Paladino, 1960). Unambiguous resolution of this quench problem requires accurate experiments at temperature rather than on quenched specimens, which is at present beyond our capability: we therefore leave open the question of whether these highest temperature samples (>1000 °C) have preserved the equilibrium cation distribution during the quench.

Nonstoichiometric magnesioferrite

Figure 2 also shows selected lattice parameters measured on samples of the nonstoichiometric magnesioferrite, quenched after annealing at temperatures between 500 and 1200 °C for various times. These experiments fall into three series, denoted A, B, and C.

For series A, a batch of the original synthesis material was reheated to 1100 °C and then quenched. The XRD pattern of this material showed almost no trace of α-Fe_2O_3. Small amounts of this material were then reheated at intervals of 100 °C from 600 to 1200 °C for 5 min and quenched. The lattice parameters define a trend with temperature that is subparallel to that established for the stoichiometric $MgFe_2O_4$ and is most likely due to the same cause, reordering of Mg and Fe^{3+}, perhaps complicated by some additional redistribution of vacancies and any Fe^{2+}. The experiments at 900 and 1000 °C that plot off the trend clearly show some exsolved α-Fe_2O_3 in their diffraction traces, indicating that perceptible exsolution of some of the excess Fe_2O_3 occurs in less than 5 min at these temperatures.

Series B used the original synthesis material, equilibrated for comparatively long times before quenching, to determine the points at which α-Fe_2O_3 ceases to exsolve at 600–900 °C (experiments varied from 10 d at 600 °C to 24 h at 900 °C).

Series C (Fig. 3) is a detailed study at 500 °C. The secular change of a_0 shows two trends: a rapid initial decrease in a_0 caused by the cation (± vacancy) redistribution, followed by a much slower increase in a_0 as excess Fe_2O_3 exsolves. The appearance and growth of coexisting α-Fe_2O_3 can be clearly seen in the XRD patterns. The final value of a_0 for this material is ~0.0013 Å lower than that for the stoichiometric material. There are several possible reasons: (1) There is still some nonstoichiometry in equilibrium with excess Fe_2O_3, even at 500 °C. (2) There is a metastable equilibrium due to the high surface free energy of the fine-grained exsolved Fe_2O_3. (3) Our stoichiometric $MgFe_2O_4$ has in fact some excess MgO (e.g., 1%, as implied by EMP and ICP analyses), and this excess is accompanied by an increase in a_0 over truly stoichiometric material. (4) The kinetics of Fe_2O_3 exsolution become prohibitively sluggish as the material approaches stoichiometry. The data in Figure 2 also suggest that the maximum amount of excess Fe_2O_3 (i.e., in equilibrium with α-Fe_2O_3) increases rapidly above 900 °C—this is very like what was found in the system Fe_3O_4-Fe_2O_3 (Dieckmann, 1982).

The importance of these observations in the present context is that they suggest that magnesioferrite synthesized with an Fe_2O_3-excess stoichiometry at high temperatures might show an a_0 vs. T curve with a trend subparallel to that shown for stoichiometric $MgFe_2O_4$ in Figure 2, the displacement of the curve to lower a_0 values depending on the amount of excess Fe_2O_3. However, this trend would be lost if the samples were annealed for long periods of time because of exsolution of α-Fe_2O_3.

Figure 4 shows a comparison of previous determinations of a_0 vs. T, with the present results. The data of Allen (1966) agree well with ours. There are some other points of agreement with the work of Allen which are worth mentioning: (1) The change in the color of $MgFe_2O_4$ from red brown at low temperatures to nearly black at high temperatures, the transition being put by Allen at 950 °C, although we observed it at 1050 °C. (2) Allen used three starting compositions, one with excess MgO, and observed no difference in the resulting products. (3) Allen was unable to produce any further change in order by annealing at temperatures below ~450 °C, as would be expected from our observations on the rate of ordering of stoichiometric $MgFe_2O_4$ at these low temperatures.

The a_0 vs. T curve of Mozzi and Paladino (1963) on what they called nonstoichiometric magnesium ferrite (with a composition given as $Mg_{1.06}Fe_{1.94}O_{3.97}$) is also similar to ours. We believe that this is additional evidence that the Mozzi and Paladino material was in fact nearly stoichiometric $MgFe_2O_4$. It is also apparent that their sample at 410 °C (annealed for only 92 h) has not quite reached equilibrium—again as expected from this study.

The data of Tellier (1967) and Faller and Birchenall (1970) plot at lower a_0 for any given temperature. In fact, both studies plot below the curve for our nonstoichiometric magnesioferrite, which probably represents the composition with the maximum amount of excess Fe_2O_3 between 1000 and 1100 °C. Given the rapid exsolution of excess Fe_2O_3 that we observe at lower temperatures (e.g., at 500 °C) from our relatively large crystals, maintaining this implied amount of nonstoichiometry would appear difficult. In the case of Tellier's study, at least, the

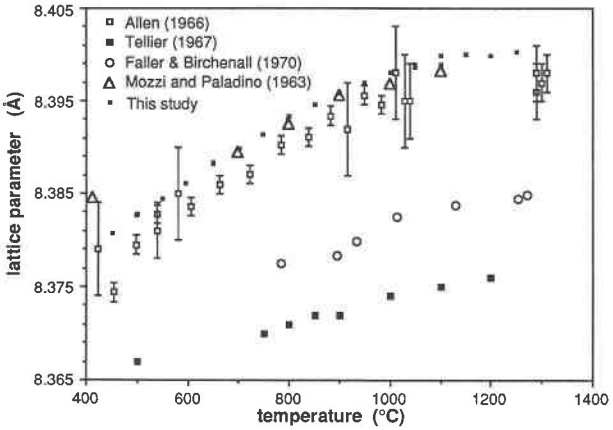

Fig. 4. A comparison of the present lattice parameter measurements on quenched $MgFe_2O_4$, with previous determinations, plotted as a function of the annealing temperature. The study of Allen (1966) is in fair agreement with our work; that of Mozzi and Paladino (1963) on what they assert was MgO-excess magnesioferrite ($Mg_{1.06}Fe_{1.94}O_{3.97}$) is in exact agreement with our data for "stoichiometric" $MgFe_2O_4$, including two details: (1) their sample at 410 °C has apparently not reached equilibrium, as expected after annealing for only 90 h; and (2) their two data at 1000 and 1100 °C plot slightly to the low side of the curve, indicating difficulty in quenching from high temperature (see Fig. 12 below). The data of Tellier (1967) and of Faller and Birchenall (1970) define subparallel trends at lower a_0 values, consistent with their material being nonstoichiometric toward γ-Fe_2O_3 (cf. Fig. 2).

discrepancy appears not to be due to any systematic error in the determination of a_0, as his results for $MgGa_2O_4$ and Mg_2TiO_4 agree reasonably well with measurements at the Bayerisches Geoinstitut (O'Neill, unpublished data).

Powder XRD structural refinements

X-ray powder diffraction intensities were measured using the same diffractometer used for the lattice constant determinations, but with Mo$K\alpha_1$ radiation ($\lambda = 0.709\,300$ Å) over the range 7–80° 2θ. Using the shorter wavelength radiation compresses the XRD pattern to a smaller range of 2θ, which has the advantages that more peaks can be measured and that less time is wasted scanning the background between peaks. Corrections for sample displacement and absorption are also less at low angles. The potential problem of peak overlap is not a severe one for spinels, as their high symmetry makes for an XRD powder pattern with relatively few peaks. Data were collected over five consecutive scans, which could then be examined for systematic drift in the intensity of the X-ray source with time. When such drift was small or negligible, the scans were then summed. This procedure also serves to even out any short-term intensity fluctuations.

Crystal structure refinements were made using two superficially rather different methods—see O'Neill et al. (1991) for a fuller discussion. In the first method (a two-stage process of profile fitting followed by structure factor minimization), integrated intensities, and the estimated errors of these intensities for each individual observable peak were obtained by fitting short segments of the summed pattern with a peak profile computer program supplied with the diffractometer. "Lorentzian-squared" or Pearson VII peak shapes were found to produce the best fits out of the peak shape options available (the others were simple Lorentzian and Gaussian). The former option was selected, as it contains fewer adjustable parameters while producing almost as good a fit. The measured intensities were used as input in a conventional least-squares crystal-structure analysis program, Simp (W. A. Dollase, unpublished data), which fits the crystal structure parameters to the appropriately weighted data.

The second method used a Rietveld-type refinement of the whole diffraction pattern, using the program DBW (Wiles and Young, 1981). Following the procedure in O'Neill et al. (1991), most of the background was subtracted from the measured pattern before inputting the data into the refinement program. Peak profiles were fitted with a Pearson VII function, in which the exponent, m, could vary as a function of 2θ ($m = a + b/2\theta$), and to which an asymmetry parameter was added for peaks below 34° 2θ. We included a correction factor to allow for sample displacement. This correction factor, the 2θ zero point, and the lattice parameter are all so highly correlated over our relatively limited range of 2θ that the lattice parameters from these refinements are not reliable. The complete set of parameters (i.e., structural and profile fitting) from one refinement are given in Table 3, by way of an example.

Apart from the different ways of fitting the peak shapes,

Table 3. Structure refinements using the Rietveld method: a summary of the model for the 750 °C/2 sample

Parameter	Background subtracted	Raw data—background not subtracted
a_0 (Å)*	8.4023(6)	8.4005(5)
2θ zero	−0.0146(3)	−0.0113(3)
Sample displacement	0.299(10)	0.263(8)
B_{tet} (Å²)	0.317(19)	0.331(18)
B_{oct} (Å²)	0.384(17)	0.397(16)
B_{ox} (Å²)	0.530(35)	0.498(31)
x	0.794(4)	0.797(3)
u	0.2563(2)	0.2565(2)
Scale	2.92(1)E-4	2.93(1)E-4
Peak half width**		
U	0.0378(18)	0.0407(15)
V	−0.0285(12)	−0.0304(10)
W	0.0137(2)	0.0142(2)
Peak profile†		
N_A	1.45(4)	1.57(4)
N_B	5.31(83)	5.09(88)
Asymmetry	0.953(46)	1.610(54)
R_p	9.49	5.37
R_{wp}	14.17	7.26
R_{Bragg}	2.11	2.43
R_F	3.67	4.71

Note: Mo$K\alpha_1$ radiation, 2θ from 7 to 80°. Refinements are given for (1) data with most of the background first subtracted and (2) the raw data.

* Not thought to be accurate—see text.

** FWHM² = $U \tan^2\theta + V \tan\theta + W$.

† Pearson VII, with $m = N_A + N_B/2\theta$.

the same X-ray structural models were used with both refinement methods. The space group $Fd3m$ was assumed, with the 8a, 16d cation sites and 32e O sites all fully occupied. Refined crystallographic parameters were a scale factor; the O positional parameter, u; the inversion parameter, x; and either one, two, or three isotropic temperature factors, B. The model with only one temperature factor (i.e., for both the cation sites and the O atoms, called here the "1B model") produced a markedly inferior fit in all cases (R factors increase by 1–2%), and will not be further considered except to note that it also caused a systematic increase in x of about 0.02 relative to that found using either the 2B or 3B models or the Mössbauer experiments. The O parameter, u, also increased by about 0.001.

The 2B model (i.e., one for both cation sites, the other for the O atoms) generally resulted in only a slightly poorer fit over the 3B model (separate temperature factors for both the cation sites and the O sites). However, the 3B model consistently produces a significant difference in the cation site isotropic temperature factors [$B_{tet} < B_{oct}$, with the difference $(B_{tet} - B_{oct}) = -0.056 \pm 0.018$ Å^2, from the Rietveld refinements, see Table 4 and Fig. 5 below]. This difference is correlated to a systematic increase in x from the 2B model of ~0.007, as compared to the results from the 3B model. In this, $MgFe_2O_4$ behaves very similarly to $NiAl_2O_4$, except that in there the relative difference in the B's is reversed, i.e., $B_{tet} > B_{oct}$ (O'Neill et al., 1991). Finally, having $B_{tet} < B_{oct}$ is consistent with the difference in the Debye temperature for Fe^{3+} in the two sites, as deduced from the recoil-free fraction effect in high-temperature (500–900 °C) Mössbauer studies (unpublished data on the present samples). We therefore adopt the 3B model with some confidence.

Final results using the 3B model and neutral atom scattering curves are given for the Simp refinements in Table 5 and for the Rietveld refinements in Table 4. For the main crystallographic parameters of interest, there is no significant difference between the two refinement methods (the mean difference in x is 0.0004 ± 0.005 and in u is 0.0001 ± 0.0002, $n = 22$). The Rietveld refinements are more precise, as judged both from estimated standard deviations and from the smoothness of the variations of x and u with temperature; that is presumably because the profile-fitting functions available with the Rietveld method are more sophisticated, in that peak profile parameters may be varied continuously with 2θ and include an asymmetry correction for the low angle reflections. The Riet-

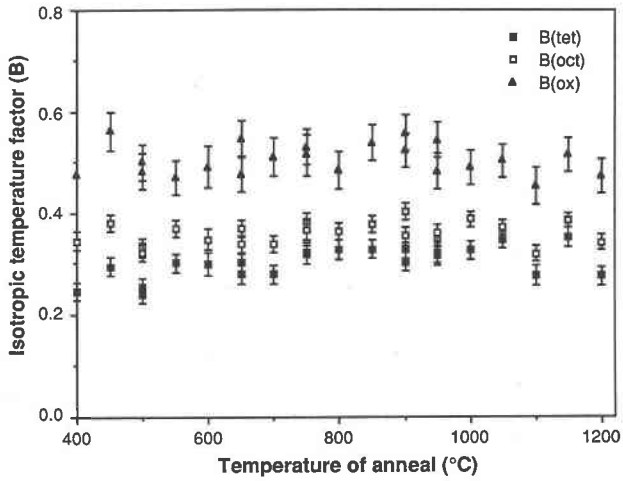

Fig. 5. Isotropic temperature factors (B_{tet}, B_{oct}, and B_{ox}) from the Rietveld refinements, plotted against the temperature of anneal. There is no change with anneal temperature, and consistently $B_{tet} < B_{oct}$.

TABLE 4. $MgFe_2O_4$ powder XRD structural refinements using the Rietveld method

Sample (T/batch)	x (±0.004)	u (±0.0002)	B_{tet}	B_{oct}	B_{ox}	R_{Bragg}	R_F
400/1*	0.899	0.2557	0.245(18)	0.345(18)	0.475(34)	2.37	3.18
450/2	0.900	0.2557	0.294(18)	0.380(18)	0.562(37)	3.16	3.99
500/1	0.884	0.2560	0.253(18)	0.322(18)	0.483(36)	2.85	3.77
500/2	0.882	0.2559	0.240(18)	0.331(17)	0.500(35)	2.99	4.48
550/2	0.869	0.2561	0.300(17)	0.368(17)	0.471(33)	2.00	3.46
600/2	0.850	0.2563	0.299(22)	0.347(21)	0.491(41)	2.02	2.98
650/1	0.832	0.2566	0.278(19)	0.338(17)	0.546(37)	3.11	4.23
650/2	0.826	0.2561	0.300(17)	0.368(17)	0.471(33)	2.49	2.89
700/2	0.811	0.2564	0.278(19)	0.337(17)	0.511(37)	2.32	3.08
750/1	0.800	0.2563	0.320(22)	0.366(19)	0.515(41)	2.86	4.09
750/2	0.794	0.2563	0.317(17)	0.384(17)	0.530(35)	2.11	3.67
800/2	0.782	0.2564	0.327(19)	0.363(17)	0.484(36)	2.72	3.61
850/2	0.772	0.2566	0.328(18)	0.377(16)	0.539(35)	2.03	3.72
900/1	0.759	0.2573	0.302(18)	0.356(16)	0.558(35)	3.63	3.20
900/2	0.757	0.2567	0.330(19)	0.402(17)	0.524(35)	2.02	3.00
950/1	0.746	0.2568	0.315(19)	0.361(16)	0.545(35)	3.43	3.22
950/2	0.749	0.2565	0.321(19)	0.347(16)	0.483(34)	2.25	3.19
1000/2	0.732	0.2565	0.326(19)	0.388(16)	0.489(34)	1.97	2.85
1050/2	0.725	0.2569	0.346(17)	0.373(14)	0.503(32)	2.34	4.13
1100/1	0.721	0.2566	0.276(20)	0.319(16)	0.454(36)	3.07	3.48
1150/1	0.719	0.2569	0.352(19)	0.386(15)	0.516(34)	2.64	3.74
1200/1	0.710	0.2569	0.275(19)	0.342(16)	0.473(34)	3.15	4.57

* Thought not to have reached equilibrium.

TABLE 5. $MgFe_2O_4$ powder XRD structural refinements using the two step method*

Sample (T/batch)	x	u	B_{tet}	B_{oct}	B_{ox}	R	w-R
400/1**	0.900(8)	0.2558(3)	0.303(17)	0.395(17)	0.588(30)	2.8	3.5
450/2	0.904(8)	0.2556(3)	0.393(20)	0.444(20)	0.748(38)	3.3	4.0
500/1	0.879(9)	0.2558(3)	0.313(19)	0.395(18)	0.622(33)	3.2	3.9
500/2	0.882(8)	0.2557(3)	0.322(19)	0.388(18)	0.695(34)	2.9	3.7
550/2	0.871(7)	0.2560(2)	0.313(19)	0.395(18)	0.622(33)	3.2	3.9
600/2	0.850(9)	0.2559(3)	0.367(24)	0.392(21)	0.687(38)	2.2	3.3
650/1	0.836(8)	0.2563(3)	0.411(19)	0.426(17)	0.699(33)	2.7	4.2
650/2	0.836(9)	0.2563(3)	0.361(22)	0.394(19)	0.663(37)	3.6	4.3
700/2	0.818(9)	0.2563(3)	0.347(20)	0.376(17)	0.610(32)	3.0	3.7
750/1	0.793(9)	0.2564(3)	0.357(22)	0.424(18)	0.671(35)	2.5	3.5
750/2	0.795(8)	0.2564(3)	0.366(19)	0.423(16)	0.663(35)	2.4	4.0
800/2	0.779(9)	0.2560(3)	0.394(23)	0.421(19)	0.687(34)	3.3	4.4
850/2	0.775(7)	0.2566(3)	0.391(20)	0.415(16)	0.683(32)	2.3	4.2
900/1	0.756(10)	0.2568(4)	0.299(25)	0.357(19)	0.610(45)	3.8	4.2
900/2	0.756(8)	0.2563(3)	0.365(22)	0.428(18)	0.651(33)	2.6	4.4
950/1	0.743(9)	0.2567(3)	0.349(21)	0.410(16)	0.645(31)	2.9	3.6
950/2	0.748(8)	0.2567(3)	0.367(22)	0.393(17)	0.607(32)	3.0	3.4
1000/2	0.734(8)	0.2564(3)	0.390(23)	0.427(17)	0.663(35)	3.0	4.1
1050/2	0.729(7)	0.2566(2)	0.370(18)	0.382(13)	0.620(26)	2.3	3.2
1100/1	0.720(9)	0.2566(3)	0.360(26)	0.387(19)	0.673(39)	3.3	4.2
1150/1	0.706(9)	0.2567(3)	0.377(19)	0.429(19)	0.691(38)	3.0	4.3
1200/1	0.702(10)	0.2566(3)	0.339(26)	0.413(19)	0.679(39)	3.4	4.7

* Profile fitting followed by structure refinement with the Simp program.
** Thought not to have reached equilibrium.

veld results will therefore be used in the following discussions. For the temperature factors, the results from the Simp refinements are consistently slightly higher, but the relative relationships are maintained (i.e., $B_{tet} < B_{oct} < B_{ox}$). Tests with the Rietveld refinement program using fully ionized scattering curves caused x to increase by ~0.001–0.008 (and thus to agree less well with the low-temperature Mössbauer results, see below), whereas u decreased by 0.0001–0.0002. There is also a tendency for the difference in B_{tet} and B_{oct} to lessen, whereas B_{ox} increases to ~0.65 (± 0.05). The calculated R factors generally increased: R_{Bragg} by ~0.5%, R_F by 0–0.2%.

Values of x and u for samples equilibrated from 450 to 1200 °C are plotted in Figure 6 as a function of the equilibration temperature. The estimated standard deviations from the refinements of x and u (±0.004 and ±0.0002) are in good agreement with estimates from the variation between experiments. For x, this is best illustrated by considering the change in a_0 with x, shown in Figure 7. With a standard deviation for x of ±0.004 and for a_0 of ±0.00015 Å, the 19 data between 400 and 1050 °C (i.e., the range in which stoichiometry is thought to be maintained) are fitted well by a straight line, with

$$x = 81.34 - 9.598a_0 \text{ (Å)}. \quad (6)$$

The reduced χ^2 for this regression is 0.536, indicating that the above esd are good estimates of the precision of the data (the reduced χ^2 is less than unity because our esd for a_0 is adjusted to include the maximum potential variation in laboratory temperature, which is not a random variable). The data at 1100 and 1150 °C fall exactly on this trend, but that at 1200 °C appears slightly offset, perhaps indicating a significant effect from nonstoichiometry by this stage. In terms of molar volumes, the above relationship may be expressed as

$$V \text{ (cm}^3\text{/mol)} = 45.799 - 1.652x. \quad (7)$$

Thus in thermodynamic terms the volume change is not large, and the effect of pressure would be virtually negligible at a few GPa.

There is no correlation between the isotropic temperature factors and degree of inversion, as shown in Figure 5 (using the results from the Rietveld refinements). The mean values for the temperature factors are $B_{tet} = 0.304 \pm 0.029$, $B_{oct} = 0.360 \pm 0.023$, and $B_{ox} = 0.507 \pm 0.031$ Å^2. These uncertainties compare well with the esd from the refinements, which average −0.019, 0.017, and 0.036 Å^2, respectively.

MÖSSBAUER SPECTROSCOPY

Conventional transmission spectra were collected in a 512 multichannel analyzer, operated in conjunction with a constant acceleration electromechanical drive unit. The symmetric ramp to the drive was generated from a specially designed circuit board in an Apple II PC. A ^{57}Co in Rh foil was used as the source, and a calibration spectrum of natural Fe at room temperature was simultaneously recorded at the other end of the vibrator unit. The two mirror-symmetric spectra typically contained 0.6–0.8 × 10^6 counts/channel.

The room temperature spectra of magnesioferrite (Néel point around 600 K) indicates that there is almost complete overlap of the magnetically split patterns due to Fe^{3+} in the distinct crystallographic sites (authors' unpublished data). In order to increase the resolution of the Mössbauer spectra, the spectral data reported in this study were

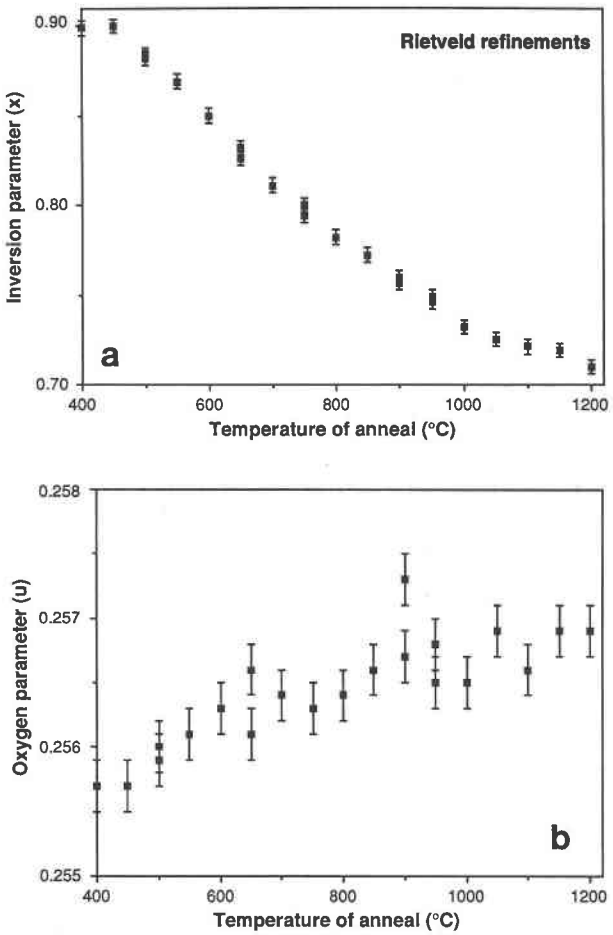

Fig. 6. Results of the powder XRD structural refinements on quenched $MgFe_2O_4$, using the Rietveld refinement method. (**a**) The inversion parameter, x, vs. temperature of anneal; (**b**) the O positional parameter, u, vs. the temperature of anneal.

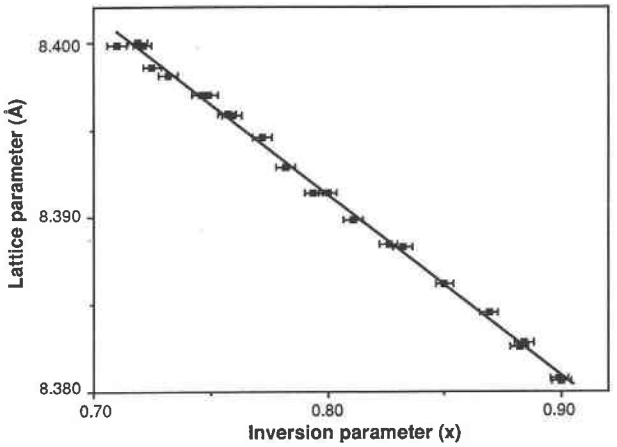

Fig. 7. Lattice parameter (a_0) vs. inversion parameter (x) from the Rietveld refinements. As well as showing the linear trend, this plot confirms that the estimated standard deviation in x from the Rietveld refinements, ± 0.004, is a realistic measure of precision.

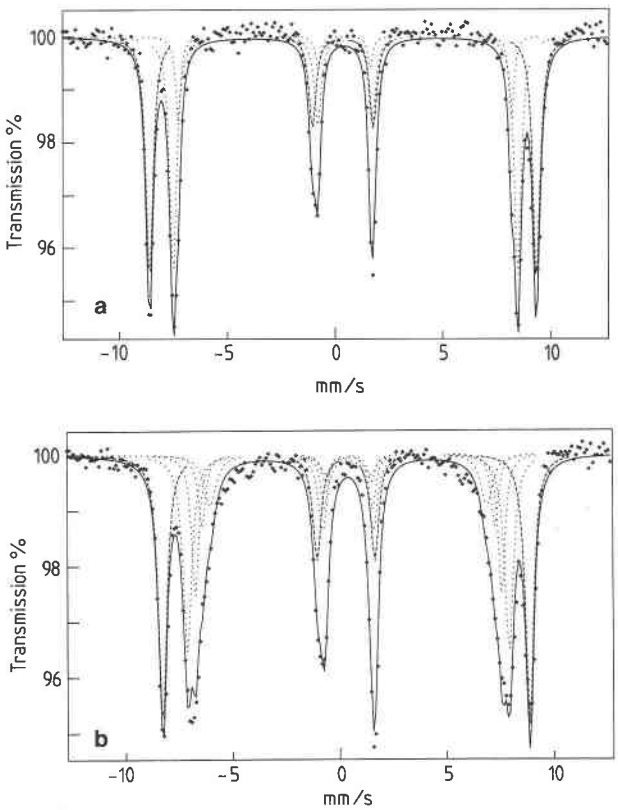

Fig. 8. Mössbauer spectra of stoichiometric $MgFe_2O_4$ measured in an external field of 4.5 T. The absorption patterns indicated by the dashed line refers to Fe^{3+} in the tetrahedrally coordinated site, and that by the dotted lines to octahedrally coordinated Fe^{3+}. (**a**) $MgFe_2O_4$ quenched from 500 °C after 8 d; absorber temperature = 189 K; (**b**) $MgFe_2O_4$ quenched from 1050 °C after 35 min; absorber temperature = 171 K.

obtained in the presence of an externally applied magnetic field using a superconducting magnet, cooled to 4.2 K to produce a magnetic field of 4.5 T. In these experiments the external magnetic field is oriented parallel to the propagation of the γ ray, and thus the intensity of the transitions, $\Delta M_I = 0$, vanish. In addition the magnetic hyperfine field at the tetrahedral site increases, while that at the octahedral site decreases. Accordingly, each six-line pattern in the 298-K spectra of $MgFe_2O_4$ is reduced to four lines in the presence of the external magnetic field, and there is almost complete resolution of the patterns due to octahedrally and tetrahedrally coordinated Fe^{3+} (Fig. 8).

Absorbers were made by mixing powdered samples of equilibrated and quenched magnesioferrite with ~100 mg of the thermosetting plastic powder, heating to 120 °C under pressure in a mold and cooling to room temperature. The absorber thickness was 7 mg of Fe per cm^2. The absorber was cooled to a low temperature in order that any difference in the recoil-free fraction that might influ-

ence the absorption areas under the respective resonance patterns, and therefore result in erroneous site occupancies, was minimized. For this reason, the spectral data were recorded with the absorber in the temperature range 12–189 K (Table 6). Since we find no systematic difference between x determined from the XRD refinements and x from the Mössbauer data at either 12 K or ~170 K (see below, e.g., Fig. 9), we conclude that the ratio of the recoilless fractions of Fe at the distinct crystal sites is close to unity in this temperature range. It can also be expected that the distribution of magnetic hyperfine fields at the octahedral site, as discussed below, will be reduced by decreasing the absorber temperature (Sawatsky et al., 1969).

The mirror-image spectral data obtained in an applied field were averaged, and the least-squares fitting of the spectra were carried out, using lines of Lorentzian shape. Fitting of the spectral data incorporated equal half-widths of each four-line pattern, and the calculated values of the inversion parameters (Table 6) were independent of whether the intensities in each pattern were unconstrained or whether the intensities of the peaks, outer: inner: inner: outer, were constrained to the theoretical values, 3:1:1:3.

The spectra of $MgFe_2O_4$ in an applied field are similar to that reported by Sawatsky et al. (1969). The absorption patterns due to Fe^{3+} in tetrahedral and octahedral coordination are readily distinguished by their characteristic isomer shift values (Table 6, Fig. 8). It is clear, however, that the outer lines of the absorption pattern due to $^{[6]}Fe^{3+}$ are asymmetrically broadened compared with those corresponding to $^{[4]}Fe^{3+}$ and also that the half-width of the Fe^{3+} (B site) absorption increases with increasing x (cf. Fig. 8). For this reason, it was necessary to fit additional hyperfine patterns corresponding to Fe^{3+} (B site) in order that the area under the accumulative envelope was adequately described. In all cases, there was a significant improvement in the goodness of fit, but the statistical criteria (χ^2) approached steady values with an increase in the number of additional patterns. For the $MgFe_2O_4$ equilibrated at 1050 °C, four hyperfine-split patterns were used to fit the absorption due to Fe^{3+} (B), but only three were necessary for the other heat-treated samples (Table 6). For all samples the absorption due to Fe^{3+} (A) was fitted to a single hyperfine pattern. The broadening of the B-site lines in $MgFe_2O_4$ has been interpreted as being due to a distribution of magnetic hyperfine fields caused by the distribution of Fe^{3+} and Mg between next-nearest A site neighbors (e.g., Sawatsky et al., 1969). On this basis, it can be expected the number of different hyperfine fields at the B site will increase with increasing x, as observed in Figure 8. No attempt was made in this study to match the number of different hyperfine fields at the B site with the calculated number of probable distributions of Fe^{3+} and Mg at the A site (Sawatsky et al., 1969).

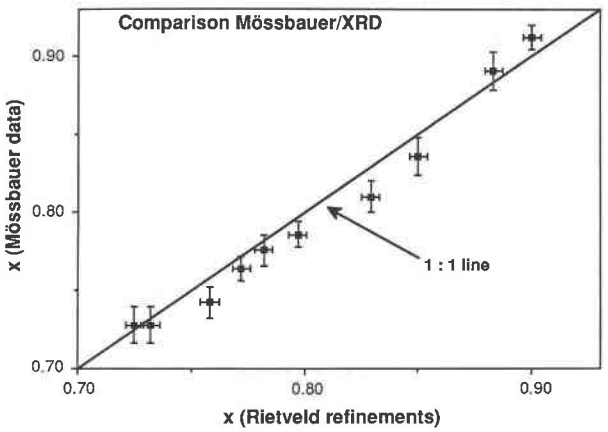

Fig. 9. Comparison of the powder XRD determinations of x from the Rietveld refinements with those from the Mössbauer data. The average deviation is 0.0056 ± 0.0102 in x. Data are plotted with 1-sd error bars.

The hyperfine parameters calculated from the Mössbauer spectra are given in Table 6. The inversion parameters are compared with those from the Rietveld refinements of the same samples in Figure 9. The average deviation in x is 0.0056, with a standard deviation of ±0.0102. Thus the Mössbauer results are in excellent agreement with XRD data. Note that this agreement would be less acceptable if we had used in our XRD model either fully ionized scattering curves or a 1B or 2B model for the isotropic temperature factors.

There have been a limited number of previous Mössbauer studies of $MgFe_2O_4$ (Sawatsky et al., 1969; De Grave et al., 1979). However, because they used a high temper-

TABLE 6. Mössbauer data for $MgFe_2O_4$

Sample (°C)	Absorber (K)	Isomer shift (mm/s)		Magnetic field (T)		Line width (mm/s)		Area fraction	
		Tet	Oct	Tet	Oct	Tet	Oct	Tet site	x
450	12	0.37(1)	0.47(1)	51.0(2)	53.5(2)	0.39(1)	0.36(2)	0.456(4)	0.912(8)
500	189	0.31(1)	0.42(1)	48.7(2)	51.0(2)	0.45(1)	0.44(2)	0.445(6)	0.890(12)
600	12	0.36(1)	0.49(1)	51.0(2)	53.3(2)	0.40(1)	0.45(2)	0.418(6)	0.836(12)
650	162	0.32(1)	0.43(1)	49.0(2)	50.5(2)	0.44(1)	0.48(2)	0.405(5)	0.810(10)
750	12	0.36(1)	0.48(1)	51.0(2)	52.7(2)	0.43(1)	0.38(2)	0.393(4)	0.786(8)
800	161	0.32(1)	0.43(1)	49.1(2)	50.5(2)	0.42(1)	0.50(2)	0.388(5)	0.776(10)
850	161	0.32(1)	0.43(1)	49.0(2)	50.2(2)	0.42(1)	0.49(2)	0.382(4)	0.764(8)
900	162	0.32(1)	0.43(1)	48.9(2)	49.8(2)	0.43(1)	0.50(1)	0.371(5)	0.742(10)
1000	12	0.37(1)	0.48(1)	51.0(2)	52.6(2)	0.43(1)	0.38(1)	0.364(6)	0.728(12)
1050	171	0.32(1)	0.43(1)	48.5(2)	48.4(2)	0.46(1)	0.47(2)	0.364(6)	0.728(12)

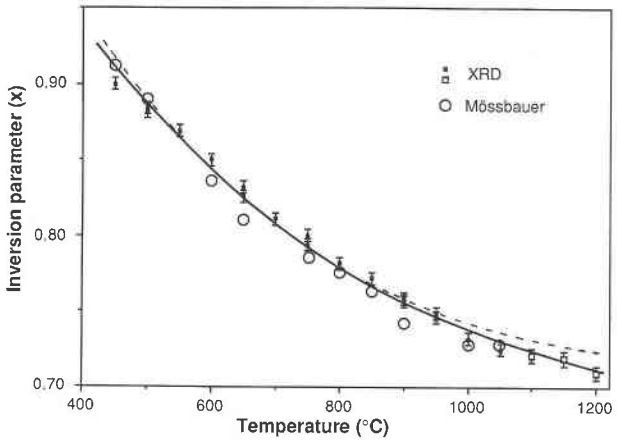

Fig. 10. A comparison of models—(1) two-term model (Eq. 8), with no excess nonconfigurational entropy of disorder (dashed curve), and (2) three-term model (Eq. 9), including an excess entropy term (unbroken curve). The XRD data are plotted with 1-sd error bars; uncertainty in the Mössbauer data is 0.008–0.012, not shown for clarity. The three XRD data from 1100 to 1200 °C (open symbols) were not included in the regressions, since these samples might be slightly O deficient, and one cannot be sure that the equilibrium cation distribution was completely preserved during quenching. Nevertheless, they plot exactly on the three-term trend, but not the two-term.

ature in their sample preparation (1400 °C), the $MgFe_2O_4$ may not be stoichiometric, as discussed above. In fact their samples, prepared from sintered oxide mixtures, probably show some excess Fe with a_0 as small as 8.373 Å for a slowly cooled magnesioferrite (De Grave et al., 1979). The inversion parameters obtained for the slowly cooled and a quenched specimen were reported to be 0.94 and 0.80 (De Grave et al., 1979) and 0.88(4) and 0.75(4) (Sawatsky et al., 1969), respectively.

Thermodynamic modeling

The Mössbauer and Rietveld powder XRD data from the samples held at 450 to 1050 °C, inclusive, were fitted by nonlinear least squares to the expression

$$-RT\ln\left(\frac{x^2}{(1-x)(2-x)}\right) = \alpha^{Mg\text{-}Fe^{3+}} + 2\beta x. \quad (8)$$

The values of x were weighted according to their estimated standard deviations: ±0.008–0.012 for the Mössbauer data (Table 6) and ±0.004 for the XRD data (Table 4). The fit gives $\alpha^{Mg\text{-}Fe^{3+}} = 26.6 \pm 0.4$ and $\beta = -21.7 \pm 0.3$ kJ/mol, $\chi^2_\nu = 1.95$. This fit is demonstrated in Figure 10. The value of χ^2_ν is slightly high, and a close look at the fit shows that the data deviate in a systematic fashion, with the data defining a straighter trend in x-T space than the calculated curve. The three data at 1100–1200 °C fall off the calculated trend. This may be due to some O deficiency and possibly also to quenching problems.

A slightly better fit is obtained with the data at 450–1050 °C if an extra term representing a nonconfigurational entropy of mixing is included, such that

$$-RT\ln\left(\frac{x^2}{(1-x)(2-x)}\right) = \alpha^{Mg\text{-}Fe^{3+}} - T\sigma^{Mg\text{-}Fe^{3+}} + 2\beta x. \quad (9)$$

We retrieve $\alpha^{Mg\text{-}Fe^{3+}} = 16.9 \pm 5.6$, $\beta = -17.3 \pm 2.5$ kJ/mol, and $\sigma^{Mg\text{-}Fe^{3+}} = -2.67 \pm 1.52$, $\chi^2_\nu = 1.10$. The data at 1100–1200 °C lie exactly on this trend (Fig. 10), even though they were not used in the fit.

This excess entropy is small and only of marginal statistical significance, given that, although we believe that the precision of our measurements has been correctly estimated (e.g., Fig. 7), there may be a slight systematic error in terms of absolute accuracy, for example due to a small degree of MgO-excess nonstoichiometry, or our choice of peak fitting procedures, or the use of the neutral atom scattering model. In addition, since there is a clear influence of cation distribution on the magnetic ordering in $MgFe_2O_4$ (see next section), the reverse should hold true in the temperature region of magnetic ordering. Such coupling might therefore cause the lowest temperature datum (which, at 450 °C, is only 77 °C above its Néel point) to deviate from the simple model. Nevertheless, it is interesting to note that the magnitude and sign of the excess entropy accords well with what might be expected from simple lattice vibration theory. For a reversible process, the change in entropy may be written

$$\delta S = \left(\frac{\partial S}{\partial V}\right)_T \delta V = \left(\frac{\partial P}{\partial T}\right)_V \delta V \quad (10)$$

and in the simplest anharmonic approximation:

$$\left(\frac{\partial P}{\partial T}\right)_V = \frac{\gamma C_V}{V} \quad (11)$$

so that

$$\delta S \approx \gamma C_V \frac{\delta V}{V} \quad (12)$$

where γ is the Gruneisen parameter, which is typically around unity for many oxides, and C_V is the heat capacity at constant volume, given in the high temperature limit by $3nR$. From the change of a_0 with x, $dV/V = -0.036$ per unit x (Eq. 7), so that we calculate $\sigma^{Mg\text{-}Fe^{3+}} \approx -6.3$ J/K·g-atom. In summary, since the molar volume of $MgFe_2O_4$ decreases slightly with x, we should perhaps expect the nonconfigurational, or lattice, entropy to increase accordingly, too.

Finally, the cation distribution in $MgFe_2O_4$ is actually quite well described using the α and β parameters estimated in O'Neill and Navrotsky (1984, their Table A1) from spinel systematics (20 and −20 kJ/mol, respectively).

Néel point measurements

The Néel temperature of $MgFe_2O_4$ is a sensitive function of cation distribution, and also of stoichiometry, and has been used by several authors (e.g., Tellier, 1967; Walters and Wirtz, 1971) as a means of characterizing their "$MgFe_2O_4$" samples. We have therefore also measured

TABLE 7. Néel temperature in quenched stoichiometric $MgFe_2O_4$, measured by DSC

T of anneal (°C)	Inversion (x)*	Néel T (°C)
500	0.883**	366.2
600	0.850	346.9
700	0.811	330.3
800	0.782	315.8
900	0.758**	303.4
1000	0.732	291.8

Note: Accuracy is estimated as ±0.5 °C (1 sd).
* From XRD Rietveld refinements.
** Average of two.

the Néel temperature of some of our samples (quenched from 500 to 1000 °C), so as to enable further comparisons with these other studies. Measurements were made with a differential scanning calorimeter (Seteram DSC 111), employed in a step-scanning mode. We scanned from 20 to 820 °C in steps of 4 °C, at a rate of 0.5 °C per min, and with an interval of 5 min between steps (for thermal equilibration). Temperature was calibrated at the same scanning rate using the melting points of In, Sn, and Pb. Results are output as heat capacities (C_P). We determined the Néel point (the maximum in a very obvious λ transition) by fitting the C_P data to two polynomials in temperature, one above and one below the maximum C_P, and determining the point of intersection. We estimate that this procedure is accurate to ±0.5° (1σ). The results are given in Table 7 and are plotted as a function of temperature of annealing and of inversion parameter (x) in Figure 11. Empirically, the Néel temperature is a quadratic function of anneal temperature, and a linear function of x.

The Néel point of Fe_3O_4 is 572 °C (e.g., Hemingway, 1990), and that of γ-Fe_2O_3 is thought to be near 675 °C (Lindsley, 1976). As a first approximation, the Néel point of a "$MgFe_2O_4$" specimen may be expected to increase monotonically toward these temperatures with increasing nonstoichiometry, and Néel point comparisons may thus be used as a sensitive test for disparities in stoichiometry. Thus the data of Tellier (1967), which we suspect to be nonstoichiometric from the lattice parameter measurements (see Fig. 4), also show significantly higher Néel temperatures (except for the 500 °C datum), and define a trend of θ_N vs. x roughly parallel to our data. The study of Epstein and Frackiewicz (1958) shows a similar displacement, though not as severe. The x vs. T results of Epstein and Frackiewicz are identical to those of Kriessman and Harrison (1956); both studies used saturation magnetization to determine x, both on samples prepared at 1400 °C. Kriessman and Harrison report a_0 measurements which indicate some nonstoichiometry (as expected from the high synthesis temperature). However, Néel temperatures reported by Kriessman (1957, unpublished data, quoted in Kriessman and Greifer, 1970), apparently using the same samples as in Kriessman and Harrison (1956), are very different from those given by Epstein and Frackiewicz. The reason for that is not known.

The high-temperature heat contents of $MgFe_2O_4$ were measured up to 1550 °C by Bonnickson (1954). He reported a phase transition at 953 °C involving a heat of

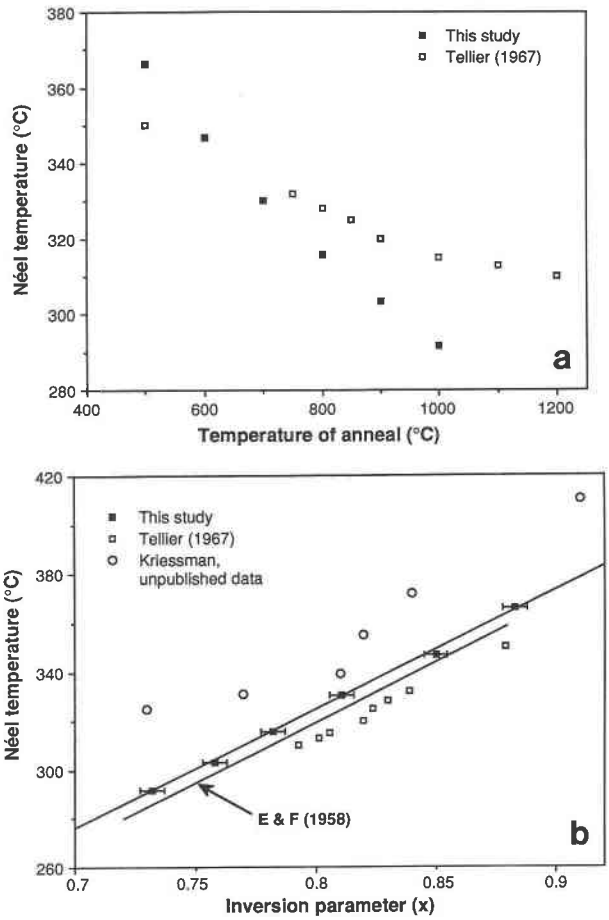

Fig. 11. Néel temperature (θ_N) of $MgFe_2O_4$, plotted against (**a**) temperature of anneal, showing a parabolic trend; and (**b**) inversion parameter (x) from the powder XRD Rietveld refinements (straight line). The latter relationship again helps to confirm that the esd of x from the Rietveld refinements (±0.004) is a realistic estimate of precision. E & F: Epstein and Frackiewicz (1958).

absorption of 1.5 kJ/mol. Since there is no evidence for any structural change in $MgFe_2O_4$ near this temperature, this "transition" might be an artifact, marking a kinetically induced change in stoichiometry. The Néel point reported by Bonnickson (392 °C, x not known) is consistent with considerable nonstoichiometry in his samples.

Comparison with previous measurements

In Figure 12 we compare our results with some previous measurements of the cation distribution in quenched samples of $MgFe_2O_4$.

None of the previous XRD studies listed in Table 1 is directly comparable with our work, since these early studies generally made use of only a few reflections and assumed the "1B model" for the temperature factors. Accordingly, these studies cannot be expected to be very precise, and may also show systematic deviations, probably of up to ±0.03 in x and 0.001 in u (see also comparisons with early powder XRD refinements of $NiAl_2O_4$ spinel in O'Neill et al., 1991). Given these limitations,

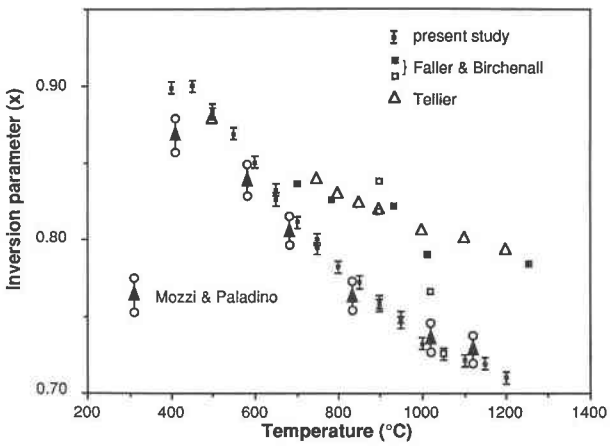

Fig. 12. Comparison of the present results on the inversion in $MgFe_2O_4$ as a function of temperature with some previous results. For simplicity, only the present XRD results (from the Rietveld refinements) are shown. The XRD results of Faller and Birchenall (1970) on both quenched specimens (filled squares) and at temperature (open squares) are shown. The data of Mozzi and Paladino (1963) are shown both as reported (lower circles) and recalculated assuming stoichiometry (upper circles, connected to lower by an arrow). Their results, when corrected, coincide with the present study from 600 to 850 °C (they are plotted displaced along the temperature axis, for clarity), with their datum at 410 °C falling below the curve, and their data at 1000 and 1100 °C above, as do also the a_0 values for these experiments—see Figure 4.

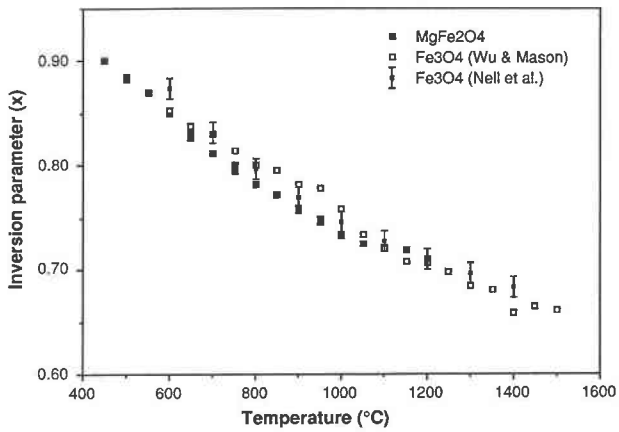

Fig. 13. Comparison of the temperature dependence of the cation distribution in quenched $MgFe_2O_4$, with that in Fe_3O_4 measured at temperature, from the thermopower (Seebeck coefficient). Error bars for the thermopower measurements of Nell et al. (1989) are plotted as ± 0.01 in x, which is approximately 25% of the uncertainty estimated by these authors. The internal consistency of the data and comparison with the measurements of Wu and Mason (1981) indicate that the original estimate is too pessimistic.

we note that the three data (at 410, 700, and 1100 °C) of Mozzi and Paladino (1963) are in good agreement with our results, particularly if it is accepted that their sample quenched from 410 °C has not quite reached equilibrium. Their value of u (0.256 ± 0.001) is also reasonable. In contrast, the results of Faller and Birchenall (1970) appear distinctly anomalous: as well as very low lattice parameters (Fig. 4), Faller and Birchenall report unrealistically low values for u, of around 0.243. The range for all 2-3 inverse spinels is 0.251–0.259 (O'Neill and Navrotsky, 1983), and such a low value would translate into a very short tetrahedral cation-O bond length; perhaps this reflects vacancies in the tetrahedral site in Faller and Birchenall's specimens. The results for x of Allen (1966) show too much scatter for any useful conclusions to be drawn.

Mozzi and Paladino (1963) also used saturation magnetization measurements to determine x for their samples. Their results in terms of x were reported under the assumption that their samples were nonstoichiometric, whereas we have argued that their samples were very probably stoichiometric. We have therefore recalculated x from their reported values of the saturation moment (μ_0), read from their Figure 4. When that is done, their results agree within the estimated uncertainties with ours, in the range 600–1000 °C, as shown in Figure 12. Their datum at 410 °C gives a slightly low x, as expected from its not having reached equilibrium and consistent with the measured a_0, whereas their datum at 1100 °C gives an x value that is very slightly too high, again as might be expected from the difficulty of quenching from this temperature.

Of the other saturation magnetization studies, that of Kriessman and Harrison (1956) gives saturation moments approximately 0.35 Bohr magnetons lower than that of Mozzi and Paladino at a given equilibration temperature. This corresponds to x values higher by ~0.035. Kriessman and Harrison also report lattice parameter measurements, which are a consistent 0.004 Å lower than ours (or Mozzi and Paladino's) at a given equilibration temperature, which might indicate that their samples contained about 5% of the γ-Fe_2O_3 component. Their samples were synthesized at 1400 °C, at which temperature thermodynamic data suggest they should have had a substantial Fe_3O_4 content (Eq. 5 above; also, cf. the measurements of the FeO content by Speidel, 1967, and Ulmer and Smothers, 1968, at 1300 °C); if the Fe_3O_4 content is accompanied by excess MgO, then on cooling or annealing at lower temperatures in air, oxidation to the γ-Fe_2O_3 component would occur, provided the excess MgO does not reequilibrate. Epstein and Frackiewicz (1958) employed the same synthesis conditions and get the same results, except for measurement of the Néel temperature.

Lastly, in Figure 13 we compare the temperature dependence of the cation distribution in Fe_3O_4, as deduced from the thermopower (Seebeck coefficient) measurements of Wu and Mason (1981) and Nell et al. (1989), with the cation distribution found for $MgFe_2O_4$ in the present study. The three curves are practically coincident and could be made even more so, were one to assume that the thermopower for Fe_3O_4 included a very small entropy-of-transport term (see Wu and Mason, 1981;

about 2 μV/K, or about 2% of the measured thermopower, would suffice). Also, the lowest temperature data for Fe_3O_4, which show the largest difference from the $MgFe_2O_4$ data, will be affected to some extent by the proximity of the Curie point in Fe_3O_4. That Fe_3O_4 and $MgFe_2O_4$ show essentially the same inversion with temperature is furthermore consistent with the thermopower plus conductivity measurements of Nell et al. (1989) on the Fe_3O_4-$MgFe_2O_4$ binary solid solution. That is not unexpected, since the systematic treatment of the oxide spinels shows that the site preference energies of Fe^{2+} and Mg are very similar; this is fortuitous, since (as pointed out by O'Neill and Wall, 1987) approximating the two as having the same site preference energy leads to a great simplification in thermodynamic modeling of compositionally complex, naturally occurring, spinel solid solutions.

Acknowledgments

We thank Michael Fleet and an anonymous reviewer for helpful reviews and Glenn Waychunas for his editorial handling. H.O'N. gratefully acknowledges his support from a Deutsche Forschungsgemeinschaft grant to Fritz Seifert.

References cited

Agranovskaya, A.I., and Saksonov, Yu.G. (1966) Crystal structure of solid solutions in the Mg_2TiO_4-$MgFe_2O_4$ systems. Soviet Physics—Crystallography, 11, 196–198.

Allen, W.C. (1966) Temperature dependence of properties of magnesium ferrite. Journal of the American Ceramic Society, 49, 257–260.

Babaev, G.Yu., Kocharev, A.G., Pokrovskii, B.I., Ptasevic, H., and Yamzin, I.I. (1976) Neutron-diffraction study of magnesium ferrite-gallates with the spinel structure. Soviet Physics—Crystallography, 21, 294–296.

Bertaut, E.F. (1951) Sur quelques progrès récents dans la crystallographie des spinelles, en particulier des ferrites. Journal de Physique et le Radium, 12, 252–255.

Blackman, L.C.F. (1959) On the formation of Fe^{2+} in the system MgO-Fe_2O_3-$MgFe_2O_4$ at high temperatures. Journal of the American Ceramic Society, 45, 143–145.

Bonnickson, K.R. (1954) High temperature heat contents of calcium and magnesium ferrites. Journal of the American Chemical Society, 76, 1480–1482.

De Grave, E., De Sitter, J., and Vandenberghe, R. (1975) On the cation distribution in the spinel system yMg_2TiO_4-$(1 - y)MgFe_2O_4$. Applied Physics, 7, 77–80.

De Grave, E., Govaert, A., Chambaere, D., and Robbrecht, G. (1979) A Mössbauer effect study of $MgFe_2O_4$. Physica, 96B, 103–110.

Dieckmann, R. (1982) Defects and cation diffusion in magnetite (IV): Non-stoichiometry and point defect structure of magnetite ($Fe_{3-\delta}O_4$). Berichte Bunsengesellschaft physikalische Chemie, 86, 112–118.

Dieckmann, R., and Schmalzried, H. (1977) Defects and cation diffusion in magnetite (II). Berichte Bunsengesellschaft physikalische Chemie, 81, 414–419.

Epstein, D.J., and Frackiewicz, B. (1958) Some properties of quenched magnesium ferrites. Journal of Applied Physics, 29, 376–377.

Faller, J.G., and Birchenall, C.E. (1970) The temperature dependence of ordering in magnesium ferrite. Journal of Applied Crystallography, 3, 496–503.

Hemingway, B.S. (1990) Thermodynamic properties for bunsenite, NiO, magnetite, Fe_3O_4, and hematite, Fe_2O_3, with comments on selected oxygen buffer reactions. American Mineralogist, 75, 781–790.

Katsura, T., and Kimura, S. (1965) Equilibria in the system FeO-Fe_2O_3-MgO at 1160 °C. Bulletin of the Chemical Society of Japan, 38, 1664–1670.

Kriessman, C.J., and Greifer, A.P. (1970) Mg-Fe^{3+} spinels (Mg ferrites) and Mg-Fe^{3+} spinels with substitutions. In K.-H. Hellwege and A.M. Hellwege, Eds., Landolt-Börnstein, magnetic and other properties of oxides and related compounds, vol. 4b, p. 216–314. Springer-Verlag, Berlin.

Kriessman, C.J., and Harrison, S.E. (1956) Cation distribution in ferrospinels; magnesium-manganese ferrites. Physical Review, 103, 857–860.

Kunnmann, W., Ferretti, A., Arnott, R.J., and Rogers, D.B. (1965) Single crystal growth of transition metal oxides from polytungstate fluxes. Journal of the Physics and Chemistry of Solids, 26, 311–314.

Lindsley, D.H. (1976) The crystal chemistry and structure of oxide minerals as exemplified by the Fe-Ti oxides. In Mineralogical Society of America Reviews in Mineralogy, 3, 1–30.

Mozzi, R.L., and Paladino, A.E. (1963) Cation distribution in non-stoichiometric magnesium ferrite. Journal of Chemical Physics, 39, 435–439.

Navrotsky, A., Wechsler, B.A., Geisinger, K., and Seifert, F. (1986) Thermochemistry of $MgAl_2O_4$-$Al_{8/3}O_4$ defect spinels. Journal of the American Ceramic Society, 69, 418–422.

Nell, J., Wood, B.J., and Mason, T.O. (1989) High temperature cation distributions in Fe_3O_4-$MgAl_2O_4$-$MgFe_2O_4$-$FeAl_2O_4$ spinels from thermopower measurements. American Mineralogist, 74, 339–351.

O'Neill, H.St.C., and Navrotsky, A. (1983) Simple spinels: Crystallographic parameters, cation radii, lattice energies, and cation distribution. American Mineralogist, 68, 181–194.

——— (1984) Cation distributions and thermodynamic properties of binary spinel solid solutions. American Mineralogist, 69, 733–753.

O'Neill, H.St.C., and Wall, V.J. (1987) The olivine-orthopyroxene-spinel oxygen geobarometer, the nickel precipitation curve, and the oxygen fugacity of the Earth's upper mantle. Journal of Petrology, 28, 1169–1191.

O'Neill, H.St.C., Dollase, W.A., and Ross, C.R., II (1991) Temperature dependence of the cation distribution in nickel aluminate ($NiAl_2O_4$) spinel: A powder XRD study. Physics and Chemistry of Minerals, 18, 302–319.

Paladino, A.E. (1960) Phase equilibria in the ferrite region of the system FeO-MgO-Fe_2O_3. Journal of the American Ceramic Society, 43, 183–191.

Pauthenet, R., and Bochirol, L. (1951) Aimentation spontanée des ferrites. Journal de Physique et le Radium, 12, 249–251.

Robie, R.A., Hemingway, B.S., and Fisher, J.R. (1978) Thermodynamic properties of minerals and related substances at 298.15 K and 1 bar (10^5 pascals) pressure and at higher temperatures. U.S. Geological Survey Bulletin 1452, 456 p.

Sawatsky, G.A., Van der Wande, F., and Mirrush, A.H. (1969) Mössbauer study of several ferrimagnetic spinels. Physical Review, 187, 747–757.

Schmalzried, H. (1961) Röntgenographische Untersuchung der Kationenverteilung in Spinelphasen. Zeitschrift für physikalische Chemie, Neue Folge, 28, 203–219.

Speidel, D. (1967) Phase equilibria in the system MgO-FeO-Fe_2O_3: The 1300 °C isothermal section and extrapolations to other temperatures. Journal of the American Ceramic Society, 50, 243–248.

Tamaura, Y., and Tabata, M. (1990) Complete reduction of carbon dioxide to carbon using cation-excess magnetite. Nature, 346, 255–256.

Tellier, J.-C. (1967) Sur la substitution dans le ferrite de magnésium des ions trivalents, tétravalents et pentavalents. Revue de Chimie Minerale, 4, 325–365.

Ulmer, G.C., and Smothers, W.J. (1968) The system MgO-Cr_2O_3-Fe_2O_3 at 1300 °C in air. Journal of the American Ceramic Society, 51, 315–319.

Walters, D.S., and Wirtz, G.P. (1971) Kinetics of cation ordering in magnesium ferrite. Journal of the American Ceramic Society, 54, 563–565.

Wiles, D.B., and Young, R.A. (1981) A new computer program for Rietveld analysis of X-ray powder diffraction patterns. Journal of Applied Crystallography, 14, 149–151.

Wu, C.C., and Mason, T.O. (1981) Thermopower measurement of cation distribution in magnetite. Journal of the American Ceramic Society, 64, 520–522.

Manuscript received July 10, 1991
Manuscript accepted March 20, 1992